Journal of Fluorescence, Vol. 7, No. 4, 1997

Scanning Near-Field Optical Microscopy and Microspectroscopy of Green Fluorescent Protein in Intact *Escherichia coli* Bacteria

Vinod Subramaniam,[1] Achim K. Kirsch,[1] Rolando V. Rivera-Pomar,[2] and Thomas M. Jovin[1,3]

Received October 27, 1997; Revised January 12, 1998; accepted January 23, 1998

Scanning near-field optical microscopy (SNOM) yields high-resolution topographic and optical information and constitutes an important new technique for visualizing biological systems. By coupling a spectrograph to a near-field microscope, we have been able to perform microspectroscopic measurements with a spatial resolution greatly exceeding that of the conventional optical microscope. Here we present SNOM images of *Escherichia coli* bacteria expressing a mutant green fluorescent protein (GFP), an important reporter molecule in cell, developmental, and molecular biology. Near-field emission spectra confirm that the fluorescence detected by SNOM arises from bacterially expressed GFP molecules.

KEY WORDS: Near-field; scanning near-field optical microscopy; fluorescence microscopy; three-dimensional imaging.

INTRODUCTION

Green fluorescent proteins (GFP) isolated from certain species of jellyfish have attracted enormous attention in recent years as important reporters in cell, developmental, and molecular biology.[1-3] GFP can be fused to a variety of proteins without affecting their function. These proteins are expressed *in vivo* and thus act as remarkably versatile indicators of structure and function within cells.[4-6] The GFP fusion proteins can be visualized and localized in cells and embryos using standard microscopy techniques;[7,8] however, the spatial resolution of conventional microscopy can be a limiting factor.[9] Nonlinear optical techniques such as multiphoton absorption[10] can enhance the ability to perceive small intracellular structures.[11] Improving resolution beyond the limits of diffraction optics is also an aim of near-field techniques. Scanning near-field optical microscopy (SNOM) offers enhanced axial and lateral resolution for topographic features and optical signals and is developing into an important technique for visualizing biological systems.[12-16] A recent report featured the detection of wild-type GFP in bacteria by SNOM.[17,18]

We have designed a SNOM system using uncoated fiber tips in the shared-aperture mode[19] for imaging biologically relevant systems in reflection and fluorescence.[20] In our own work on GFP, a mutant of the *Aequoria victoria* GFP exhibiting a red-shifted absorption peak (RSGFP), thereby facilitating efficient excitation by both the 458- and the 488-nm lines from an argon-ion laser, was expressed in *E. coli*. Topographic information and fluorescence from the intracellular GFP

[1] Department of Molecular Biology, Max Planck Institute for Biophysical Chemistry, Am Fassberg 11, D-37077 Göttingen, Germany.
[2] Department of Molecular Developmental Biology, Max Planck Institute for Biophysical Chemistry, Am Fassberg 11, D-37077 Göttingen, Germany.
[3] To whom correspondence should be addressed. Fax: +49 551 2011467. e-mail:tjovin@mpc186.mpibpc.gwdg.de.

1053-0509/97/1200-0381$12.50/0

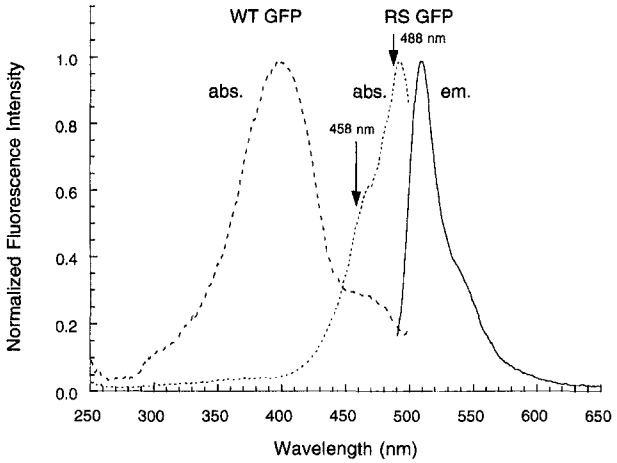

Fig. 1. Fluorescence excitation spectra of wild-type GFP and mutant RSGFP and the corresponding emission spectrum of RSGFP (λ_{ex}, 480 nm). Note that the excitation spectrum of RSGFP is red-shifted by almost 100 nm relative to wild-type GFP. The positions of the two excitation wavelengths used for SNOM measurements are marked on the RSGFP excitation spectrum.

were acquired with the SNOM instrument. Emission spectra were recorded by coupling the fluorescence signal into a spectrograph, thereby confirming the expressed protein as the origin of the optical signal. These preliminary experiments confirmed the ability to image GFP using the SNOM and are being extended to studies of the expression and colocalization of GFP fusion proteins and GFP-tagged partners in ligand–receptor interactions.

EXPERIMENTAL

GFP

A mutant (RSGFP) of the cloned *Aequoria victoria* GFP first developed by Delagrave *et al.* with combinatorial mutagenesis techniques[21] and exhibiting a red-shifted excitation spectrum relative to that of the wild-type protein (Fig. 1) was used. The principal advantage of GFP mutants with red-shifted absorption is their suitability for excitation with the 488 nm and other blue lines of an argon-ion laser, used extensively in microscopy and imaging applications. The RSGFP mutant carries the following changes in the protein sequence encompassing the chromophore: F64M, S65G, and Q69L. We amplified the RSGFP open reading frame (ORF) from the plasmid pCS-RSGFP (a gift from Dr. Enrique Amaya, Cambridge University, UK) by PCR. Appropriate primers were used to generate a *Nhe*I site at the start codon and a *Xba*I site immediately downstream of the stop codon. The digested PCR product was cloned into the *Nhe*I site of the vector pRSETa (Invitrogen, USA). The recombinant plasmid, pRS-RSGFP, allows expression of a modified RSGFP ORF containing six histidines at the amino terminus under control of the T7 promoter, which is inducible by isopropyl-β-D-thiogalactoside (IPTG). GFP-positive bacteria were selected with ampicillin. The recombinant plasmid was transformed into *E. coli* BL21 (DE3) cells. Cells were cultured in LB medium supplemented with ampicillin and grown to an $A_{600} \approx 0.6$, at which point protein expression was induced using IPTG. Cells were typically grown further for 6 h following induction.

Fluorimetry

Excitation and emission spectra were acquired on suspensions of intact cells using an SLM 8000 spectrofluorometer (SLM Instruments, Urbana, IL). For excitation spectra of both wild-type and mutant GFP, the emission was monitored at 510 nm; for the emission spectrum of RSGFP, excitation was at 480 nm.

SNOM Sample Preparation

Bacteria from a 1-ml aliquot of the induced cultures were pelleted by centrifugation at room temperature and fixed by resuspension for 10 min in phosphate-buffered saline (PBS) containing 4% paraformaldehyde. Following fixation, the bacteria were pelleted and washed three times in PBS. For SNOM samples, the fixed bacteria were pelleted and resuspended in water. Ten microliters of this suspension was placed on a freshly cleaved mica disk and the sample was air-dried.

SNOM Instrument

The near-field optical microscope used in this study was a modified version of the system described in previous reports.[19,22] The sample scanning stage and control electronics of a commercial scanning force microscope system (NanoScopeIII, Digital Instruments, Santa Barbara, CA) is coupled to a shear-force sensor head of our own design, in which an uncoated fiber tip is mounted. The fiber tip is produced from an optical fiber (Siecor, 3M, Germany) in a heating and pulling process (P-2000, Sutter Instruments, Novato, CA) and is used for both illumination of the sample and detection of the light emanating from the sample (shared aperture mode).[19,23–26] The shear-force detection system for regulating the distance between the fiber tip and the sample

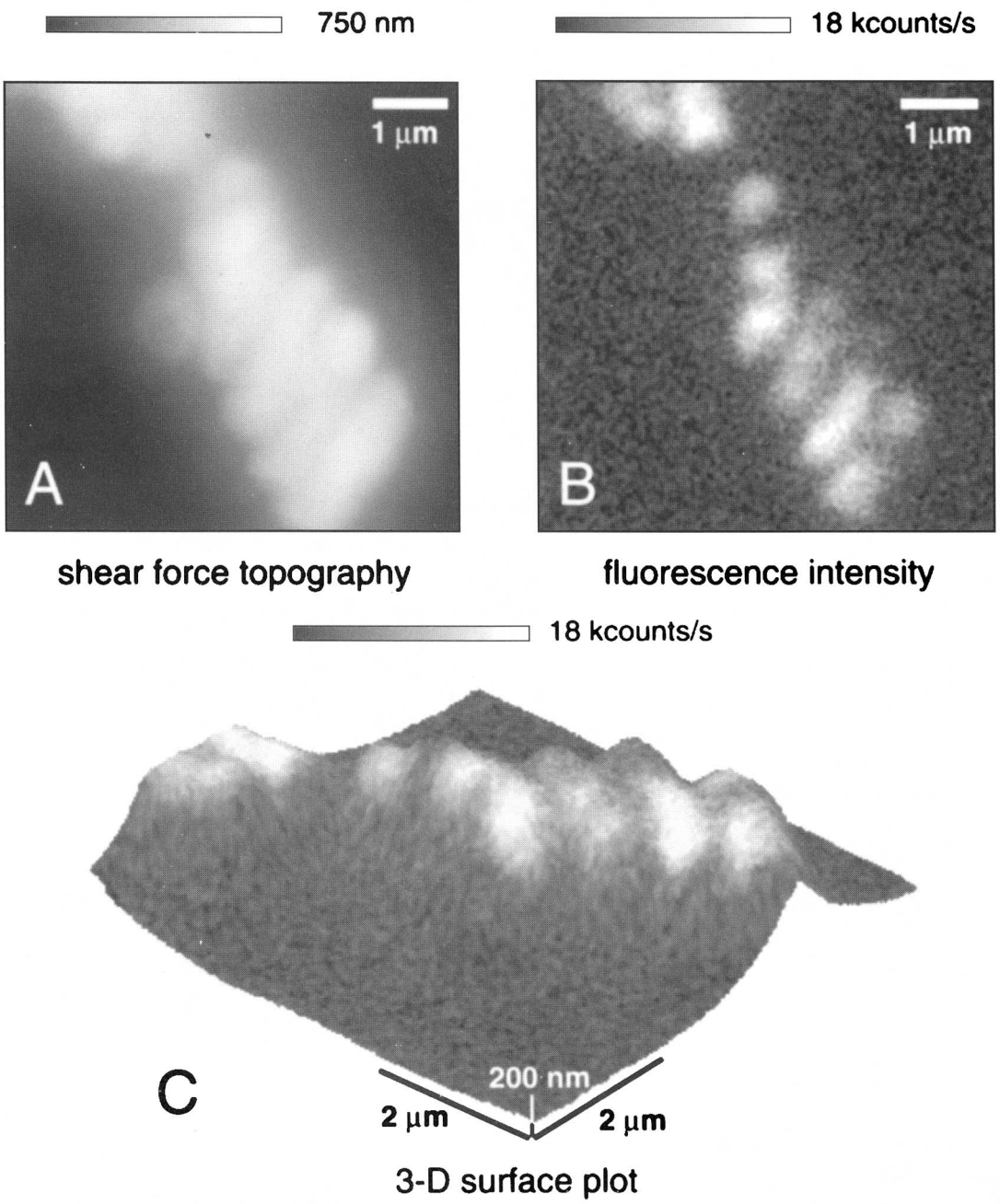

Fig. 2. Topographic (A) and near-field fluorescence (B) image of *E. coli* expressing RSGFP. λ_{exc} = 488 nm, λ_{det} = 530 ± 15 nm. Scan parameters: 0.3-Hz line frequency, 256 lines, 4.1-ms counting time/pixel, and maximum counts/pixel = 268. (C) Surface plot combining the topographic (height) and fluorescence (brightness) information. The grayscale over A codes for topographic height; the bars over B and C, for fluorescence counts (kcounts/s).

surface to 5–10 nm is similar to the configuration described in[22] but uses a 7-mW, 780-nm diode laser (SPM 780, Power Technology Inc., Little Rock, AR) for better spectral separation from the optical signals of interest.

For imaging, the 488-nm laser line of a Ar–Kr mixed gas laser (Performa, Spectra Physics, Mountain View, CA) was coupled into the fiber sensor. The fluorescence from the sample was collected with the fiber

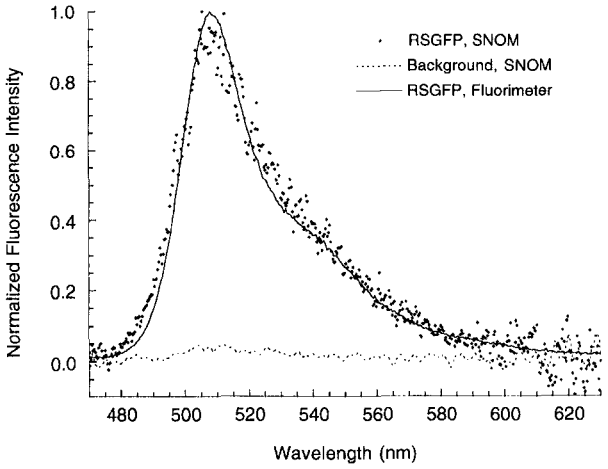

Fig. 3. Near-field spectrum (points) of bacterially expressed RSGFP acquired by positioning the fiber tip above a bright cell (λ_{ex}, 457.8 nm). The solid line is a superimposition of a conventional fluorescence spectrum from a suspension of cells expressing RSGFP (λ_{ex}, 458 nm). For reference, a background spectrum is also shown.

tip and isolated from the excitation light by means of a dichroic mirror (505 DRLP02; Omega Optical, Brattleboro, VT). Light coupling into the fiber tip from the 780-nm shear-force laser was blocked by a BG 40 filter (Schott, Germany). GFP fluorescence was selected by a bandpass filter (530DF30; Omega Optical) and detected with a single-photon counting avalanche photodiode (SPCM-AQ 131; EG&G Optoelectronics, Canada). Single-photon events were counted by the pulse counting board of the NanoScope electronics.

Near-field fluorescence spectra following excitation with the 457.9-nm laser line of the Ar–Kr laser were recorded using a beam splitter (Spindler & Hoyer, Göttingen, Germany) instead of the dichroic mirror and a 457-nm holographic notch filter (HNF-457.9-1.0; Kaiser Optical, Ann Arbor, MI). The collected light was directed by means of a beam shaping fiber optic into a spectrograph (MS125; Oriel, Stratford, CT) coupled to an intensified CCD system (InstaSpec 5, Oriel).

All measurements were performed under ambient conditions at room temperature. Images were processed with the NanoScope software and with SxMImage (CSEM, Switzerland).

RESULTS

The simultaneously recorded topographic and fluorescence images of *E. coli* cells expressing RSGFP are shown in Fig. 2. Figure 2A depicts the topography of the bacteria, color-coded for height, and Fig. 2B. shows the corresponding fluorescence signal from the bacterially expressed GFP. The optical signal reveals a distinct heterogeneous distribution of fluorescence within the bacteria, clearly evident in the bottom right quadrant as distinct variations in fluorescence intensity within each bacterium. Control samples of *E. coli* cells in which GFP expression had not been induced by the addition of IPTG showed little fluorescence. Leaky expression of the RSGFP, however, led to a weak optical signal (data not shown). Figure 2C combines the topography and fluorescence information in a surface plot grayscale encoded for the intensity of the optical signal and highlights the inhomogeneous distribution of RSGFP in the cells.

Near-field spectroscopic measurements were performed by positioning the fiber tip over a selected point on the bacterium and directing the collected light into the spectrograph. The spectrum of the collected fluorescence is depicted in Fig. 3. The solid line is a superimposition of the corrected fluorescence spectrum obtained by conventional fluorimetry. The near-field spectrum corresponded very closely to that obtained in the fluorimeter from a cell suspension, verifying that the detected fluorescence indeed arises from bacterially expressed RSGFP. For comparison purposes, we include a background spectrum, which lacked spectral features in the measurement window, as expected.

DISCUSSION

The development of GFPs as fusion tags has revolutionized the visualization and localization of target proteins in biological systems. The availability of mutants with shifted absorption and emission peaks allows for the multiple labeling required for protein colocalization measurements. In particular, the 100-nm red-shift in the excitation spectrum of RSGFP relative to wild-type GFP has been exploited to achieve dual-color microscopic imaging of the two species.[27] Although GFP can be imaged by conventional optical microscopy, SNOM methods offer enhanced spatial resolution over far-field microscopy and, in addition, provide topographical information. In our experimental configuration we are able to perform site-selective spectroscopy with unprecedented spatial resolution. For example, we demonstrated here the ability to collect fluorescence spectra from an area on the order of the effective aperture size, i.e., $\approx$200 nm in diameter. The combination of spectral and spatial resolution with selective excitation permits the precise localization of multiple fluorescent labels or fusion proteins within (or more precisely, *on*) cells. In

addition, one can use appropriately paired spectrally shifted GFP mutants for studying protein–protein interactions by fluorescence resonance energy transfer (FRET) methods, as has been demonstrated recently.[28,29] For surface-localized proteins in general and receptor–ligand interactions in particular, SNOM provides a powerful visualization technique with a resolution unmatched by other microscopies.

ACKNOWLEDGMENTS

V.S. was supported by a long-term fellowship from the Human Frontiers Science Program Organisation. A.K.K. is a graduate student of the University of Konstanz.

REFERENCES

1. M. Chalfie, Y. Tu, G. Euskirchen, W. W. Ward, and D. C. Prasher (1994) *Science* **263**, 802–805.
2. A. B. Cubitt, R. Heim, S. R. Adams, A. E. Boyd, L. A. Gross, and R. Y. Tsien (1995) *Trends Biochem. Sci.* **20**, 448–455.
3. D. C. Prasher (1995) *Trends Genet.* **11**, 320–323.
4. H. H. Gerdes and C. Kaether (1996) *FEBS Lett.* **389**, 44–47.
5. E. Yeh, K. Gustafson, and G. L. Boulianne (1995) *Proc. Natl. Acad. Sci. USA* **92**, 7036–7040.
6. M. Chalfie (1995) *Photochem. Photobiol.* **62**, 651–656.
7. K. D. Niswender, S. M. Blackman, L. Rohde, M. A. Magnuson, and D. W. Piston (1995) *J. Microsc.* **180**, 109–116.
8. J. F. Presley, N. B. Cole, T. A. Schroer, K. Hirschberg, K. J. M. Zaal, and J. Lippincott-Schwartz (1997) *Nature* **389**, 81–85.
9. H. R. B. Pelham (1997) *Nature* **389**, 17–19.
10. W. Denk, J. H. Strickler, and W. W. Webb (1990) *Science* **248**, 73–76.
11. R. H. Kohler, J. Cao, W. R. Zipfel, W. W. Webb, and M. R. Hanson (1997) *Science* **276**, 2039–2042.
12. E. Betzig, R. J. Chichester, F. Lanni, and D. L. Taylor (1993) *Bioimaging* **1**, 129–135.
13. R. C. Dunn, E. V. Allen, S. A. Joyce, G. A. Anderson, and X. S. Xie (1995) *Ultramicroscopy* **57**, 113–117.
14. H. Muramatsu, N. Chiba, T. Umemoto, K. Homma, K. Nakajima, T. Ataka, S. Ohta, A. Kusumi, and M. Fujihira (1995) *Ultramicroscopy* **61**, 265–269.
15. L. K. Tamm, C. Bohm, J. Yang, Z. F. Shao, J. Hwang, M. Edidin, and E. Betzig (1996) *Thin Solid Films* **285**, 813–816.
16. N. F. Van Hulst and M. H. P. Moers (1996) *IEEE Eng. Med. Biol.* **15**, 51–57.
17. E. Tamiya, S. Iwabuchi, N. Nagatani, Y. Murakami, T. Sakaguchi, K. Yokoyama, N. Chiba, and H. Muramatsu (1997) *Anal. Chem.* **69**, 3697–3701.
18. H. Muramatsu, N. Chiba, T. Ataka, S. Iwabuchi, N. Nagatani, E. Tamiya, and M. Fujihira (1996) *Opt. Rev.* **3**, 470–474.
19. A. K. Kirsch, C. K. Meyer, H. Huesmann, D. Möbius, and T. M. Jovin (1998) *Ultramicroscopy* **71**, 295–302.
20. A. Kirsch, C. Meyer, and T. M. Jovin (1996) in E. Kohen and J. G. Hirschberg (Eds.), *NATO Advanced Research Workshop: Analytical Use of Fluorescent Probes in Oncology, Miami, Fl*, Plenum Press, New York, pp. 317–323.
21. S. Delagrave, R. E. Hawtin, C. M. Silva, M. M. Yang, and D. C. Youvan (1995) *BioTechnology* **13**, 151–154.
22. A. K. Kirsch, C. K. Meyer, and T. M. Jovin (1997) *J. Microsc.* **185**, 396–401.
23. S. I. Bozhevolnyi, M. Xiao, and O. Keller (1994) *Appl. Opt.* **33**, 876–880.
24. H. Bielefeldt, I. Horsch, G. Krausch, M. Lux-Steiner, J. Mlynek, and O. Marti (1994) *Appl. Phys. A Solids Surf.* **59**, 103–108.
25. A. Jalocha, M. H. P. Moers, A. G. T. Ruiter, and N. F. van Hulst (1995) *Ultramicroscopy* **61**, 221–226.
26. M. Spajer, D. Courjon, K. Sarayeddine, A. Jalocha, and J. M. Vigoureux (1991) *J. Phys. III* **1**, 1–12.
27. T. T. Yang, S. R. Kain, P. Kitts, A. Kondepudi, M. M. Yang, and D. C. Youvan (1996) *Gene* **173**, 19–23.
28. A. Miyawaki, J. Llopis, R. Heim, J. M. McCaffery, J. A. Adams, M. Ikura, and R. Y. Tsien (1997) *Nature* **388**, 882–887.
29. R. D. Mitra, C. M. Silva, and D. C. Youvan (1996) *Gene* **173**, 13–17.